small method
www.small-methods.com

Dictating High-Capacity Lithium–Sulfur Batteries through Redox-Mediated Lithium Sulfide Growth

Meng Zhao, Hong-Jie Peng, Jun-Yu Wei, Jia-Qi Huang, Bo-Quan Li, Hong Yuan, and Qiang Zhang*

Regulating the solid product growth is critical for achieving high capacities in rechargeable batteries based upon multiphase and multielectron dissolution–precipitation chemistries (e.g., lithium–sulfur chemistry). The intrinsic redox mediators, polysulfides, are insufficient for effective regulation due to the dynamically changed species and concentration. Herein cobaltocene ($CoCp_2$) is introduced as a persistent extrinsic redox mediator to dictate an alternative growing pathway toward three-dimensional lithium sulfide growth, which enables at most 8.1 times enhancement in discharge capacities at harsh conditions of high-rate (>1 C) or electrolyte-lean operation (electrolyte/sulfur ratio of 4.7 µL mg_S^{-1}). The faster kinetics and higher diffusivity of $CoCp_2$ play an essential role in regulating lithium sulfide growth and increasing discharge capacities. This work not only illustrates an effective strategy to increase the capacity of high-rate or electrolyte-lean lithium–sulfur batteries but also paves a way toward the rational design of novel redox mediators for dissolution–precipitation energy chemistries.

The capacity of rechargeable batteries that operate upon dissolution–precipitation chemistries is strongly correlated to the electrodeposition/growth of solid products.[1] For instance, the growth of lithium sulfide (Li_2S) on discharge of a lithium–sulfur (Li–S) battery accounts for at least three fourth of the theoretical capacity, i.e., 1254 of 1672 mAh g_S^{-1}, in routine ether-based electrolytes.[2] The soluble intermediates, lithium polysulfides (Li_2S_n, $3 < n \leq 8$), serve as intrinsic redox mediators to guide the growth of insulating Li_2S via electroreduction on the current collectors and subsequent chemical decomposition/disproportionation.[3] Nevertheless, the limited solubility and small diffusivity of short-chain polysulfides (Li_2S_n, $n < 4$) and Li_2S/Li_2S_2 restrain the full liquid–solid conversion at the end of discharge.[4,5] Especially when operated in conditions such as at high current densities or with low electrolyte/sulfur (E/S) ratios that are practically preferred, the growth of Li_2S is always ceased due to large voltage polarization originating from the intrinsic yet sluggish mediation from polysulfides.[6]

To surmount above challenge, a variety of heterogeneous mediators have been designed and introduced to tune Li_2S electrodeposition via chemisorption and/or surface catalysis.[7] However, the effect of these immobile mediators is mainly restrained within a short distance along the perpendicular direction to the surface.[8] The capacity is somewhat dependent to the overall conductive surface area. One interesting approach to decouple the relationship between capacity and conductive surface is to engineer the speciation and properties of polysulfides in electrolytes.[9] For instance, Lu's team systematically investigated electrolyte solvents and unveiled various physicochemical properties that affect Li_2S solubility/mobility and consequently its growth morphologies.[10] Kim and colleagues employed high-donicity salt anions to implement a similar concept but demonstrated less corrosion on the lithium metal anode than high-donicity solvents.[11] Different from the dissolution–precipitation Li–S chemistry, Nazar and co-workers demonstrated an alternative quasi-solid-state pathway based upon fully coordinated salt/solvent pairs, achieving stable batteries with a low E/S ratio.[12] Despite the above advances in electrolyte engineering, we should also note their limitation in compromised kinetics that require either low current densities or high temperature (e.g., 55 °C) for battery operation. Another approach is to adopt an extrinsic redox mediator other than polysulfides to assist the redox mediation of Li_2S growth. For example, Helms and co-workers designed several imide-based redox mediators for Li–S chemistry to achieve promising high capacities.[13] Aurbach and co-workers introduced oxidizing redox mediators to recover most of Li_2S theoretical capacity in the initial activation and reduce the overpotential to

M. Zhao, J.-Y. Wei, Prof. J.-Q. Huang
School of Materials Science and Engineering
Beijing Institute of Technology
Beijing 100081, China
E-mail: jqhuang@bit.edu.cn

M. Zhao, J.-Y. Wei, Dr. H. Yuan, Prof. J.-Q. Huang
Advanced Research Institute of Multidisciplinary Science
Beijing Institute of Technology
Beijing 100081, China

Dr. H.-J. Peng, B.-Q. Li, Dr. H. Yuan, Prof. Q. Zhang
Beijing Key Laboratory of Green Chemical Reaction Engineering and Technology
Department of Chemical Engineering
Tsinghua University
Beijing 100084, China

The ORCID identification number(s) for the author(s) of this article can be found under https://doi.org/10.1002/smtd.201900344.

DOI: 10.1002/smtd.201900344

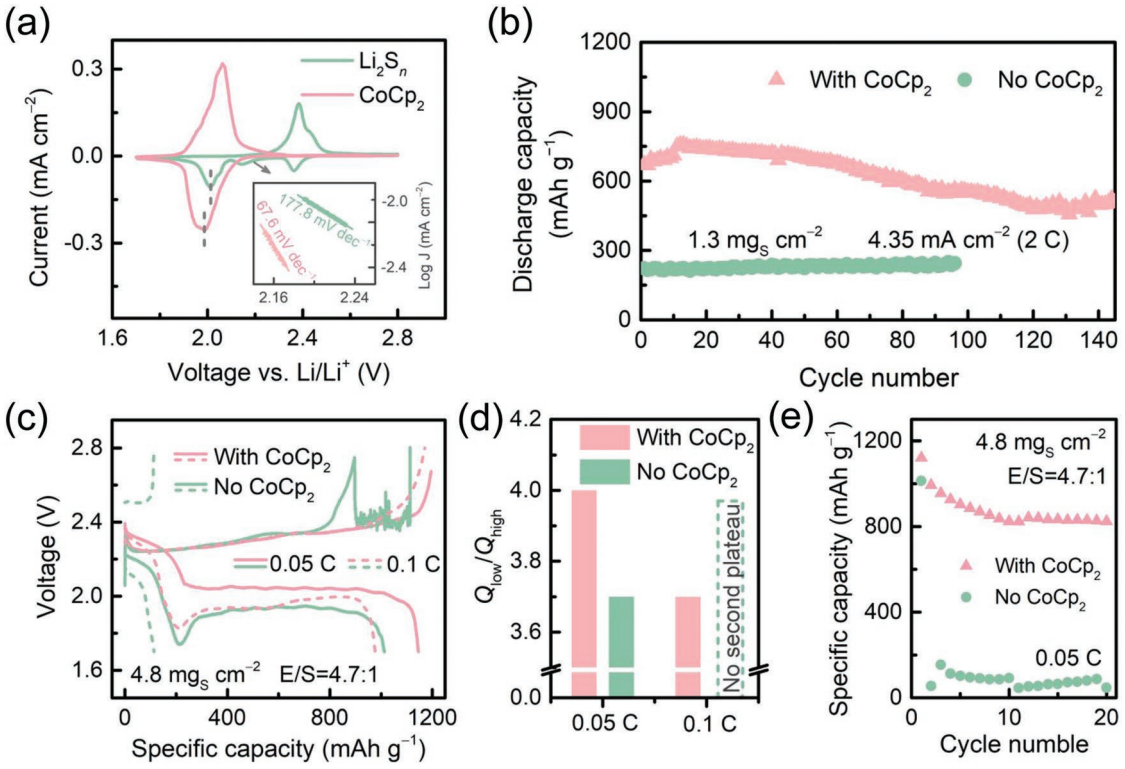

Figure 1. Electrochemical performance of Li–S batteries. a) CVs of Li|Li_2S_4 and Li|$CoCp_2$ cells with isoelectronic quantities at a scan rate of 0.1 mV s^{-1} (inset: Tafel plots for reduction reactions of Li_2S_n and $CoCp_2$). b) Cycling performance of a Li–S cell at 2 C. c) Galvanostatic discharge–charge profiles at various current densities. d) Q_{low}/Q_{high} of each Li–S cell in (c). e) Cycling performance of a Li–S cell at 0.05 C. Areal sulfur loadings (mg_S cm^{-2}) in (b), 1.3; (c–e), 4.8. E/S ratios (μL mg_S^{-1}) in (b), 16; (c–e), 4.7.

2.9 V.[14] Along with other redox mediators designed for Li–S chemistry (e.g., metallocene, quinone, and iodide),[15] these redox mediators were generally proved in an "electrolyte-flooded" cell (e.g., mostly flow cells); whereas their capability of modulating Li_2S growth in more practical electrolyte-lean conditions has rarely been investigated.

In this Communication, small-molecule cobaltocene ($CoCp_2$) was introduced as an extrinsic redox mediator to dictate a solution growing pathway for Li_2S. $CoCp_2$ transforms the deposition mode of Li_2S from two-dimensional (2D) to three-dimensional (3D) growth, thus maximizing the utility of coctive surface. The oxidized form (RM^+) of $CoCp_2$, $CoCp_2^+$, is reduced to $CoCp_2$ (RM) at a given potential, diffuses in the electrolyte, and chemically reduces residual polysulfides. Concurrently, it is chemically oxidized to $CoCp_2^+$ for continuous polysulfide reduction until polysulfides are consumed out and $CoCp_2$ remains in its reduced form before electrooxidation on charge. Since $CoCp_2/CoCp_2^+$ maintains a soluble state across the whole discharge process, it never encounters the problem as intrinsic redox mediators (namely polysulfides) that the amount and concentration of redox mediators changes constantly and so drastically at the end of discharge to no longer mediate the Li_2S growth and consequently cease it. Therefore, the persisted presence of extrinsic redox mediator ensures the integrity of redox-mediated Li_2S growth cycle toward full utilization of sulfur on the finite conductive surface. Besides, benefiting from better diffusivity and large solubility than short-chain polysulfides, $CoCp_2$ enabled high-capacity Li–S batteries both at high rates and electrolyte-lean conditions.

Metallocene with a π-bonded sandwich structure is widely used as redox mediators in dye-sensitized solar and photoelectrochemical cells due to its air stability, excellent electrochemical reversibility, and adjustable redox characteristics.[16] In order to probe the mediation mechanism, Li_2S_4 (in a nominal stoichiometry) and $CoCp_2$ catholytes with isoelectronic quantities were assembled with lithium metal anodes in coin cells, denoted as Li|Li_2S_4 and Li|$CoCp_2$ cells, respectively.

In the cyclic voltammogram (CV) of Li|Li_2S_4 cell starting from the open-circuit voltage of 2.29 V, the nominal Li_2S_4 catholyte first exhibited a small reduction peak at 2.14 V and then a major reduction peak at 2.01 V (**Figure 1**a). The first peak corresponds to the reduction of relatively stable higher-order polysulfides (e.g., Li_2S_6 or in equilibrium a trace amount of $LiS_3^{\bullet}$ radical) to more insoluble ones (e.g., Li_2S_4); while the second peak is in accordance with the formation of Li_2S. During the reverse scan, the Li_2S oxidation peak appears at 2.38 V and the huge gap between these reductive/oxidative peaks indicate the high irreversibility of Li_2S formation/oxidation. By contrast, the CV of Li|$CoCp_2$ cell exhibits highly symmetric peaks that are attributed to highly reversible $CoCp_2$ reduction/oxidation. Besides the reversibility, the comparison between CVs of Li_2S_4 and $CoCp_2$ reveals at least two additional attributes of $CoCp_2$ that should play an essential role in its redox mediation:

- The reduction peak of $CoCp_2$ is ≈27 mV more negative than the formation peak of Li_2S, suggesting that $CoCp_2$ is slightly more reducible than Li_2S. That attribute lays the thermodynamic foundation of the reaction, $CoCp_2^+ + Li_2S_n \rightarrow CoCp_2 + Li_2S$.
- Despite the more negative onset and peak potentials, the $CoCp_2/CoCp_2^+$ redox couple possesses a significantly lower Tafel slope of 67.6 than 177.8 mV dec^{-1} for the high-/low-order polysulfide couple(s), forecasting the faster electrochemical conversion kinetics of extrinsic $CoCp_2/CoCp_2^+$ than intrinsic polysulfides (inset of Figure 1a).

Consequently, $CoCp_2$ is a thermodynamically viable and kinetically favorable extrinsic redox mediator in a working Li–S battery.

Benefiting from the above attributes, $CoCp_2$ endowed Li–S cells excellent rate performance as validated by galvanostatic discharge–charge profiles at high current densities (Figure S1, Supporting Information). At 1 C (1 C = 1672 mA g_S^{-1}; 2.18 mA cm^{-2}), the discharge voltages of both cells with or without $CoCp_2$ addition are comparable at high-plateau and the beginning of low-plateau region. However, the $CoCp_2$-free cell suffers from gradual voltage decay after ≈1/4 depth of the low plateau, indicating the inefficacy of intrinsic redox mediators in mediating Li_2S growth; whereas the cell with $CoCp_2$ maintains relatively flat voltage profile across nearly the whole low-plateau region, attaining a 1/3 longer plateau than the $CoCp_2$-free cell. As the current density increases to 2 C, the cell with $CoCp_2$ preserves the two-plateau discharge profiles despite the larger voltage polarization than at 1 C. By contrast, the $CoCp_2$-free cell losses the whole low-plateau discharge characteristic due to the excessive overpotential for Li_2S formation although its high-plateau voltage is still comparable to the $CoCp_2$-containing cell. The sharp difference in low-plateau rather than high-plateau discharge voltage mainly stems from the distinct ability of intrinsic polysulfides and extrinsic $CoCp_2$ in mediating Li_2S growth at high rates.

The remarkable mediating ability of $CoCp_2$ is also long lasting. At 2 C, the capacity of the $CoCp_2$-containing cell reached its maximum of 757 mAh g_S^{-1} after activation and the cyclic capacity decay rate was 0.27% (relative to the maximum) during nearly 100 cycles (Figure 1b). $CoCp_2$ itself could only provide a capacity of less than 4 mAh g_S^{-1}, proving that the increase of discharging capacity mainly comes from the deposition of Li_2S mediated by $CoCp_2$ (Figure S2, Supporting Information). This high-rate cycling performance is much better than the $CoCp_2$-free cell with an average capacity of merely 232 mAh g_S^{-1}. Note that such an improvement only costs a tiny increase in the battery load, which is ≈0.3 % of the electrolyte weight. Nevertheless, the capacity of cells decayed more quickly due to severe shuttle when the concentration of $CoCp_2$ is increased (Figure S3, Supporting Information). Similarly, the mobility of $CoCp_2$ inevitably caused corrosion of anode Li, especially at low current density (Figure S4, Supporting Information). Therefore, to maximize the role of redox mediator, it is necessary to match effective anode protection measures.

Examining the ability of $CoCp_2$ under an electrolyte-lean rather than flooded condition is more promising yet more challenging achieve practically acceptable energy density.[17] With a limited amount of electrolyte to solvate the intrinsic redox mediators of polysulfides, the redox mediator-mediated growth of Li_2S would suffer from extremely severe overpotential that stems from the lack of redox mediators in terms of both amount and mobility; while the direct electrodeposition of Li_2S is limited by its very poor conductivity.

Herein, the E/S ratio was controlled to 4.7 μL mg_S^{-1}, a fairly low value for coin cells considering the large dead volume. At this condition, $CoCp_2$ enabled substantial reduction in the voltage polarization (Figure 1c). The $CoCp_2$-free cell possesses a significant voltage "dip" of 198 mV before low voltage plateau despite the comparable capacity before this "dip" to that of the $CoCp_2$-containing cell at 0.05 C (0.40 mA cm^{-2}). Such a huge voltage "dip" corresponds to an extremely high barrier for initial Li_2S nucleation with limited polysulfide supply. However, with the regulation by $CoCp_2$ redox mediator, not only does the initial voltage "dip" disappear but also the discharge capacity increases from 1010 to 1148 mAh g_S^{-1}. The effect of extra $CoCp_2$ mediation is more profound at 0.1 C. The initial voltage "dip" for the $CoCp_2$-free cell becomes insurmountable, hindering the formation of Li_2S; while the $CoCp_2$-containing cells are still featured with a long discharge plateau.

The ratio of low- and high-plateau capacities (Q_{low}/Q_{high}) is often used to quantitate the conversion efficiency of polysulfide-to-Li_2S. A well-accepted theoretical value of Q_{low}/Q_{high} is 3.0 in an electrolyte-flooded condition, where all polysulfides could get solvated. This value, however, is usually higher under electrolyte-lean conditions due to incomplete solvation of polysulfides and prior precipitation of Li_2S. In this sense, the $CoCp_2$-containing cell has a higher Q_{low}/Q_{high} (4.0 at 0.05 C and 3.7 at 0.1 C) than the $CoCp_2$-free cell (3.7 at 0.05 C and 0 at 0.1 C), demonstrating the significantly promoted Li_2S precipitation with the presence of an extrinsic redox mediator (Figure 1d). As a result, the extrinsic $CoCp_2$ mediators allow the electrolyte-lean cells to maintain capacity of more than 800 mAh g_S^{-1} at 0.05 C for 20 cycles (Figure 1e). On the contrary, the discharge product polysulfide cannot be completely dissolved due to lack of electrolyte, especially after the consumption of the first cycle. Therefore, the first discharge process of cells without $CoCp_2$ cannot be completely performed, and capacity of less than 200 mAh g_S^{-1} was provided.

The effect of $CoCp_2$ in Li_2S growth is further elucidated by the deposition morphologies of Li_2S at different depths of discharge (**Figure 2**a). For ease of characterization by scanning electron microscopy (SEM), carbon paper (CP) was employed as the substrate for deposition. A thin layer of flocculent Li_2S deposits appeared on CP (Figure 2b) at the initial stage of Li_2S growth. When the capacity reached 354 mAh g_S^{-1}, Li_2S maintained lamellar growth along the boundaries of previously formed precipitates, featuring a conventional 2D growth mode in low-donicity ether-based electrolytes (Figure 2c);[4] these 2D deposits merged into a fully covered film on CP that blocked the underneath conductive surface at the very end of discharge and thus further growth of insulating Li_2S (Figure 2d). In this case, the capacity is correlated to the thickness of Li_2S film, which is, however, limited by the low conductivity, solubility, and mobility of Li_2S. The declined voltage in Figure 2a is also in good accordance with the decrease in overall conductive surface.

The introduction of $CoCp_2$ altered the Li_2S growth mode significantly. At the initial stage, there were isolate fungi-like Li_2S deposits with a lateral size of 0.3–1.0 μm and a thickness of >0.3 μm (Figure 2e); then these deposits further coalesced to form larger yet porous lichen-like sediments but there was

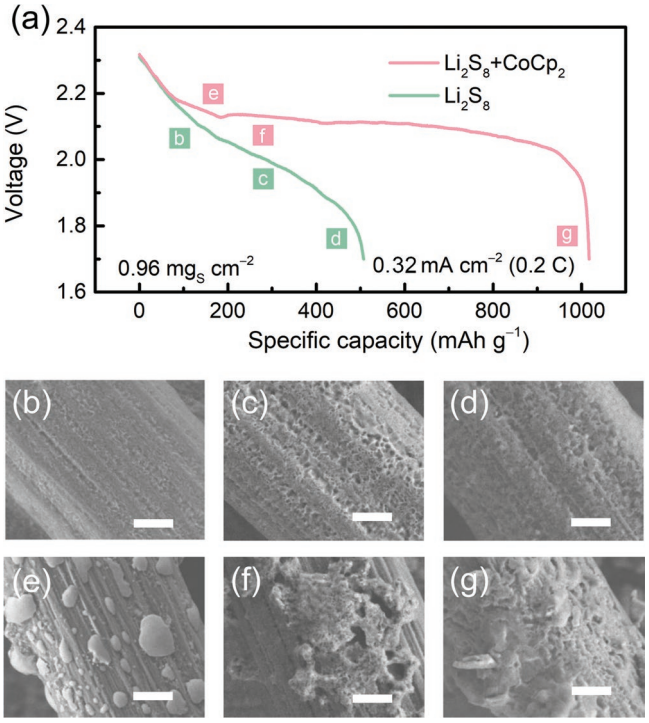

Figure 2. Li_2S growth on CP. a) The first discharge profile at 0.2 C. Cells were stopped at different depths of discharge indicated as points b–g) to characterize the Li_2S deposits. (b–g) SEM images of Li_2S deposits on CP with $CoCp_2$ absent (up, b–d) and present (down, e–g). Scale bars are 1 µm.

still sufficient naked conductive surface, in contrast to the $CoCp_2$-free case at the same stage (Figure 2f); thick terrace-like deposits were obtained at the end owing to the 3D growth of Li_2S that occurred not only on the CP surface but also along its radial direction (Figure 2g). The thicker Li_2S film corresponds to ≈100% higher capacity than that obtained without $CoCp_2$. Furthermore, it can be observed that $CoCp_2$ did not affect the crystal structure while altering the growth mode of Li_2S (Figure S5, Supporting Information).

To understand the unique electrochemical behaviors with $CoCp_2$ and rationalize necessary attributes for a good redox mediator on discharge, several experiments were designed. Metallocenes having similar structures to $CoCp_2$, such as nickelocene ($NiCp_2$) and 1,1′-bis(diphenylphosphino)ferrocene (DPPF), were employed as extrinsic redox mediators. However, they did not exhibit any redox activity within the electrochemical window of Li–S batteries and thus even deteriorated battery performance (Figure S6, Supporting Information). The sharp contrast of $NiCp_2$ and DPPF to $CoCp_2$ again indicates that a suitable redox potential is the prerequisite of everything. The same to ferrocene,[18] despite used in Li–S systems, it could only act as chemical adsorbent without any mediated activity due to excessively high potentials.[19] A slightly lower redox potential of $CoCp_2$ than Li_2S formation (≈2.0 V) not only guarantees the reductive ability of redox mediators but also not lowers the working voltage too much.

The high capacity dictated by a mobile redox mediator is hypothetically ascribed to (1) the persistency of redox mediator on whole discharge to fully utilize unreacted polysulfides and/or (2) the 3D growth of Li_2S that allows higher amount of deposition on the substrate with a certain surface area. The first hypothesis was supported by $CoCp_2$-mediated Li_2S growth on a "dead" cathode (fully discharged with no $CoCp_2$, **Figure 3**a). Fresh Li_2S_4- and $CoCp_2$-containing electrolytes with isoelectronic quantities (corresponding to a theoretical capacity of 3.6 mAh g^{-1} with respect to the sulfur weight in the "dead" cathode) were injected in cells for further discharge. The

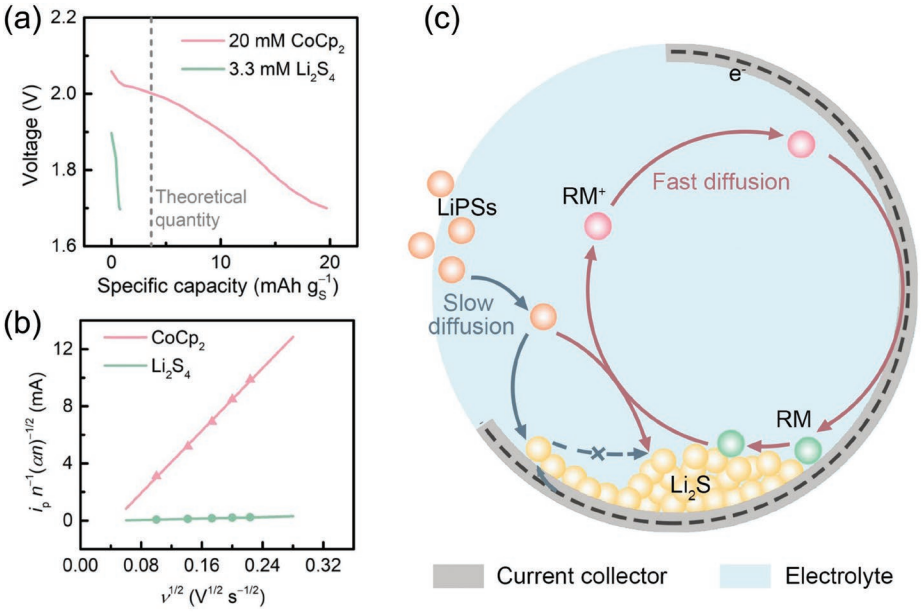

Figure 3. Mechanistic insights into the redox mediation by $CoCp_2$. a) Galvanostatic discharge curves of "dead" cells injected with fresh Li_2S_4 and $CoCp_2$ electrolyte. b) $i_p\, n^{-1/2}(\alpha n)^{-1/2}$ versus $v^{1/2}$ plots (see parameter abbreviations in the Supporting Information) for reduction peaks of Li_2S_4 and $CoCp_2^+$. The scan rates are between 10 and 50 mV s^{-1}. c) Schematic illustration of the growing pathway of Li_2S in the absence (blue arrows) and presence (red arrows) of $CoCp_2$. Li_2S grows through the solution path mediated by fast-diffusion $CoCp_2$ without directly contacting with the conductive surface.

injection of fresh Li_2S_4 electrolyte hardly contributed to further discharge but $CoCp_2$ enabled an extra capacity of 19.7 mAh g_S^{-1} on a "dead" cathode, equivalent to 5.5 times of its own charge quantity. This result unambiguously demonstrates the ability of $CoCp_2$ to chemically reduce unreacted polysulfides.

The second hypothesis was supported by the measuring diffusivity through CV at different scan rates (Figure S7, Supporting Information), which is critical for the growth behavior of Li_2S.[5] The incremental peak potential difference with scan rate is attributable to the intervention of charge-transfer step and indicates the mass-transfer limitation. Using the well-known Randles–Sevcik equation (see Supporting Information), the peaks corresponding to the reduction of Li_2S_4 and $CoCp_2$ are selected to fit the diffusion coefficients (D_{LS} and D_{CC}), respectively. Despite the difference in electron transfer number, the true D_{LS} (3.2×10^{-8} cm^2 s^{-1}) is still three orders of magnitude lower than D_{CC} (5.7×10^{-5} cm^2 s^{-1}) (Figure 3b). Therefore, $CoCp_2$ with higher diffusivity should possess at least two advantages over intrinsic RMs of polysulfides: (1) $CoCp_2^+$ has easier access to the conductive surface than Li_2S_4, especially at the end of discharge, to break the diffusion limitation on Li_2S_4 for further discharge; (2) $CoCp_2$, once formed through on-surface electroreduction, can diffuse to external surface of existing Li_2S nuclei and build new mass upon these nuclei while polysulfides like Li_2S_4 can only mediate the Li_2S growth at the electrolyte/conductive substrate/Li_2S triple-phase boundaries (Figure 3c). Besides, $CoCp_2$ has a lower polarity thus faster migration than polysulfides considering the adsorption on the strongly polar Li_2S surface. The difference in diffusivity explains the transition from 2D Li_2S growth to 3D growth after the mediation by $CoCp_2$.

In summary, we describe redox-mediated Li_2S growth by $CoCp_2$ to dictate high-capacity Li–S batteries at high rates (>1 C) or with lean electrolyte (E/S ratio: 4.7 μL mg_S^{-1}). Unlike intrinsic redox mediators of polysulfides, extrinsic $CoCp_2$ provides a persistent function on reducing polysulfides and mediating the Li_2S growth, and alters the deposition mode of Li_2S from 2D to 3D growth, thus resulting in at most 8.0 times enhancement in discharge capacities. This proof-of-concept work not only illustrates a strategy to increase the battery capacity at harsh conditions but also rationalizes several crucial principles for on-discharge redox mediator design: (1) thermodynamically a suitable redox potential (slightly lower than the product formation), (2) high diffusivity for better kinetics, (3) certain solubility to allow electrolyte-lean operation, and (4) low molecular weight to reduce the weight load. Along with other strategies for the whole cell engineering, more reliable Li–S batteries for practical applications can be prospected.

Supporting Information

Supporting Information is available from the Wiley Online Library or from the author.

Acknowledgements

M.Z., H.-J.P., and J.-Y.W. contributed equally to this work. This work was supported by the National Key Research and Development Program (2016YFA0202500 and 2016YFA0200102), National Natural Science Foundation of China (21776019, 21825501, and U1801257), and Beijing Key Research and Development Plan (Z181100004518001).

Conflict of Interest

The authors declare no conflict of interest.

Keywords

electrocatalysis, lithium sulfide nucleation, lithium–sulfur batteries, polysulfide redox reaction, redox mediator

Received: May 7, 2019
Revised: May 22, 2019
Published online: June 7, 2019

[1] a) P. G. Bruce, S. A. Freunberger, L. J. Hardwick, J. M. Tarascon, *Nat. Mater.* **2012**, *11*, 19; b) C. Xia, C. Y. Kwok, L. F. Nazar, *Science* **2018**, *361*, 777; c) S. Chu, Y. Cui, N. Liu, *Nat. Mater.* **2017**, *16*, 16; d) N. B. Aetukuri, B. D. McCloskey, J. M. Garcia, L. E. Krupp, V. Viswanathan, A. C. Luntz, *Nat. Chem.* **2015**, *7*, 50; e) X. W. Gao, Y. H. Chen, L. Johnson, P. G. Bruce, *Nat. Mater.* **2016**, *15*, 882.

[2] a) S. H. Chung, C. H. Chang, A. Manthiram, *Adv. Funct. Mater.* **2018**, *28*, 1801188; b) Z. W. Seh, Y. M. Sun, Q. F. Zhang, Y. Cui, *Chem. Soc. Rev.* **2016**, *45*, 5605; c) R. P. Fang, S. Y. Zhao, Z. H. Sun, D. W. Wang, H. M. Cheng, F. Li, *Adv. Mater.* **2017**, *29*, 1606823; d) S. Y. Lang, R. J. Xiao, L. Gu, Y. G. Guo, R. Wen, L. J. Wan, *J. Am. Chem. Soc.* **2018**, *140*, 8147; e) S. H. Chung, A. Manthiram, *Joule* **2018**, *2*, 710; f) J. Lee, J. Song, H. Lee, H. Noh, Y. J. Kim, S. H. Kwon, S. G. Lee, H. T. Kim, *ACS Energy Lett.* **2017**, *2*, 1232.

[3] a) Z. W. Zhang, H. J. Peng, M. Zhao, J. Q. Huang, *Adv. Funct. Mater.* **2018**, *28*, 1707536; b) H. J. Peng, J. Q. Huang, X. Y. Liu, X. B. Cheng, W. T. Xu, C. Z. Zhao, F. Wei, Q. Zhang, *J. Am. Chem. Soc.* **2017**, *139*, 8458.

[4] F. Y. Fan, W. C. Carter, Y. M. Chiang, *Adv. Mater.* **2015**, *27*, 5203.

[5] H. L. Pan, J. Z. Chen, R. G. Cao, V. Murugesan, N. N. Rajput, K. S. Han, K. Persson, L. Estevez, M. H. Engelhard, J. G. Zhang, K. T. Mueller, Y. Cui, Y. Y. Shao, J. Liu, *Nat. Energy* **2017**, *2*, 813.

[6] a) F. Y. Fan, Y. M. Chiang, *J. Electrochem. Soc.* **2017**, *164*, A917; b) M. R. Kaiser, S. L. Chou, H. K. Liu, S. X. Dou, C. S. Wang, J. Z. Wang, *Adv. Mater.* **2017**, *29*, 1700449; c) Q. L. Zou, Z. J. Liang, G. Y. Du, C. Y. Liu, E. Y. Li, Y. C. Lu, *J. Am. Chem. Soc.* **2018**, *140*, 10740; d) S. Chen, F. Dai, M. L. Gordin, Z. X. Yu, Y. Gao, J. X. Song, D. H. Wang, *Angew. Chem., Int. Ed.* **2016**, *55*, 4231; e) Y. X. Yang, Y. R. Zhong, Q. W. Shi, Z. H. Wang, K. N. Sun, H. L. Wang, *Angew. Chem., Int. Ed.* **2018**, *57*, 15549.

[7] a) H. B. Lin, S. L. Zhang, T. R. Zhang, H. L. Ye, Q. F. Yao, G. W. Zheng, J. Y. Lee, *Adv. Energy Mater.* **2018**, *8*, 1801868; b) X. Liang, C. Y. Kwok, F. Lodi Marzano, Q. Pang, M. Cuisinier, H. Huang, C. J. Hart, D. Houtarde, K. Kaup, H. Sommer, T. Brezesinski, J. Janek, L. F. Nazar, *Adv. Energy Mater.* **2016**, *6*, 1501636; c) M. Zhao, H. J. Peng, Z. W. Zhang, B. Q. Li, X. Chen, J. Xie, X. Chen, J. Y. Wei, Q. Zhang, J. Q. Huang, *Angew. Chem., Int. Ed.* **2019**, *58*, 3779; d) C. Ye, Y. Jiao, H. Y. Jin, A. D. Slattery, K. Davey, H. H. Wang, S. Z. Qiao, *Angew. Chem., Int. Ed.* **2018**, *57*, 16703.

[8] a) Q. Pang, X. Liang, C. Y. Kwok, L. F. Nazar, *Nat. Energy* **2016**, *1*, 16132; b) J. B. Park, S. H. Lee, H. G. Jung, D. Aurbach, Y. K. Sun, *Adv. Mater.* **2018**, *30*, 1704162.

[9] a) G. Zhang, H. J. Peng, C. Z. Zhao, X. Chen, L. D. Zhao, P. Li, J. Q. Huang, Q. Zhang, *Angew. Chem., Int. Ed.* **2018**, *57*, 16732;

b) A. Gupta, A. Bhargav, A. Manthiram, *Adv. Energy Mater.* **2018**, 1803096.
[10] Z. J. Li, Y. C. Zhou, Y. Wang, Y. C. Lu, *Adv. Energy Mater.* **2019**, *9*, 1802207.
[11] H. Chu, H. Noh, Y. J. Kim, S. Yuk, J. H. Lee, J. Lee, H. Kwack, Y. Kim, D. K. Yang, H. T. Kim, *Nat. Commun.* **2019**, *10*, 188.
[12] Q. Pang, A. Shyamsunder, B. Narayanan, C. Y. Kwok, L. A. Curtiss, L. F. Nazar, *Nat. Energy* **2018**, *3*, 783.
[13] a) L. C. Gerber, P. D. Frischmann, F. Y. Fan, S. E. Doris, X. Qu, A. M. Scheuermann, K. Persson, Y. M. Chiang, B. A. Helms, *Nano Lett.* **2016**, *16*, 549; b) Y. Hwa, P. D. Frischmann, B. A. Helms, E. J. Cairns, *Chem. Mater.* **2018**, *30*, 685.
[14] S. Meini, R. Elazari, A. Rosenman, A. Garsuch, D. Aurbach, *J. Phys. Chem. Lett.* **2014**, *5*, 915.
[15] a) K. R. Kim, K. S. Lee, C. Y. Ahn, S. H. Yu, Y. E. Sung, *Sci. Rep.* **2016**, *6*, 32433; b) Y. Tsao, M. Lee, E. C. Miller, G. P. Gao, J. Park, S. C. Chen, T. Katsumata, H. Tran, L. W. Wang, M. F. Toney, Y. Cui, Z. N. Bao, *Joule* **2019**, *3*, 872; c) J. F. Li, L. Q. Yang, S. L. Yang, J. Y. Lee, *Adv. Energy Mater.* **2015**, *5*, 1501808; d) Z. J. Li, G. M. Weng, Q. L. Zou, G. T. Cong, Y. C. Lu, *Nano Energy* **2016**, *30*, 283.
[16] a) T. Daeneke, T. H. Kwon, A. B. Holmes, N. W. Duffy, U. Bach, L. Spiccia, *Nat. Chem.* **2011**, *3*, 211; b) J. H. Wu, Z. Lan, J. M. Lin, M. L. Huang, Y. F. Huang, L. Q. Fan, G. G. Luo, Y. Lin, Y. M. Xie, Y. L. Wei, *Chem. Soc. Rev.* **2017**, *46*, 5975.
[17] L. Cheng, L. A. Curtiss, K. R. Zavadil, A. A. Gewirth, Y. Shao, K. G. Gallagher, *ACS Energy Lett.* **2016**, *1*, 503.
[18] Y. Y. Mi, W. Liu, K. R. Yang, J. B. Jiang, Q. Fan, Z. Weng, Y. R. Zhong, Z. S. Wu, G. W. Brudvig, V. S. Batista, H. H. Zhou, H. L. Wang, *Angew. Chem., Int. Ed.* **2016**, *55*, 14818.
[19] Y. Ding, Y. Zhao, Y. Li, J. B. Goodenough, G. Yu, *Energy Environ. Sci.* **2017**, *10*, 491.